Preprints of the 21st IFAC World Congress (Virtual)
Berlin, Germany, July 12-17, 2020

Controller Design Method for Stroke Reduction of Micro-actuator in HDD

Shota Yabui * **Takenori Atsumi** ** **Tsuyoshi Inoue** ***

* *Nagoya University, Nagoya, 464-8603, Japan (e-mail: e-mail:yabui@nuem.nagoya-u.ac.jp).*
** *Chiba Institute of Technology, Narashino, 275-0016 Japan (e-mail:takenori.atsumi@p.chibakoudai.jp).*
*** *Nagoya University, Nagoya, 464-8603, Japan (e-mail: e-mail:inoue.tsuyoshi@nagoya-u.jp).*

Abstract: For realizing high information society, recording capacity of the hard disk drives (HDDs) is required to increase. The capacity of the HDDs depends on positioning accuracy of magnetic head which read/write the digital data on disks. To improve the positioning accuracy, the head positioning control system employs a dual-stage actuator system. The dual-stage actuator system is consisting of the voice coil motor (VCM) and the micro-actuator. The micro-actuator has possibility to move accurately the magnetic head in higher frequency. On the other hand, the stroke limitation can be problem for increasing the control bandwidth: improvement of the positioning accuracy. Especially, the stroke limitation is a major constraint to compensate for low frequency vibration. There is the tradeoff between the stroke limitation and the positioning accuracy. To overcome the problem, this study proposes the controller design method for stroke reduction of the micro-actuator. The proposed design method can adjust the main working frequency for each actuator. In this system, the VCM can mainly compensate for the low frequency vibration. The micro-actuator mainly focuses on stabilization of the control system in higher frequency, the working doesn't require the large stroke. The effectiveness is verified in the compensation of the representative internal and external vibration. The proposed method can reduce the stroke of the micro-actuator by about 60% with comparison to the conventional design method with keeping the positioning accuracy.

Keywords: Hard disk drives, Positioning control, Stroke reduction, Micro-actuator, Disturbance compensation.

1. INTRODUCTION

Internet of things (IoT) is the key technology in fourth industrial revolution. [Bettiol (2017)]. The IoT is supported by the cloud computing network which is including of the large amount of digital data. The digital data is mainly stored in the data-servers, and they are building rapidly by the various internet companies [SPECTRA (2017)]. The data server consists of a large number of hard disk drives (HDDs) [Yamato (2016)]. Although the current HDDs can store the large amount of digital data, capacity of the HDDs are required to be increasing by about 30% at every year for development of the data-servers.

The recording capacity depends on the positioning accuracy of the head positioning control system [Yamaguchi (2012)]. The positioning accuracy determines physical data size per one bit on the disk. To achieve the high precision control, the control system employs a dual-stage actuator system. Representitive combination of the actuators in the dual-stage actuator system is voice coil motor (VCM) and a milli actuator or VCM and a micro actuator [HGST (2017)]. The micro actuator is preferred in the positioning accuracy, because the main resonance frequency of the micro actuator is higher than that of the milli actuator. On the other hand, the stroke limitation is more severe in the controller design, because the physical size of the micro-actuator is smaller than that of the milli actuator [Bhushan (2004)].

Decouple controller design is representative design method for the dual-stage actuator system [Kobayashi (2004); Ito (2018); Bashash (2018)]. The design method can eliminate the interaction between the VCM and the micro actuator in the head positioning control. The entire control loop can be handled as two single-input-single-output (SISO) systems connected in series. The major HDD maker employs the decouple controller design in the actual head positioning system [HGST (2017)]. However, the previous studies indicate the stroke limitation is the major problem to design the controller for the micro-actuator [Bhushan (2004); Atsumi (2019); Yabui (2020)]. Especially, the controller gain should be increased to compensate for low frequency vibration (less than 2kHz) which worsen the positioning accuracy. Although the micro-actuator is required to move for compensation of the vibration, the stroke limitation is constraint for the compensation. There is trade-off between the positioning accuracy and the stroke limitation.

Authors propose a novel controller design method for the stroke reduction of the micro-actuator. The proposed method employs the high gain controller for the VCM

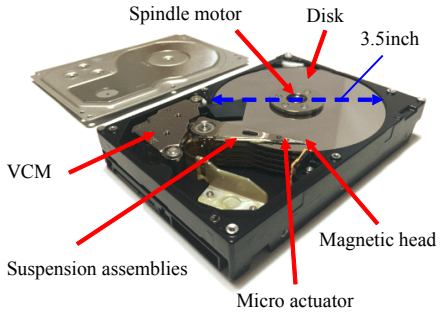

Fig. 1. Picture of components of the HDD

feedback loop. The VCM feedback loop can be unstable in the high frequency range. The micro-actuator feedback loop focuses on stabilization of the entire feedback loop in high frequency range. In this condition, the main working frequency can be distinguished for each actuator. The vibration in higher frequency tend to be smaller than that of lower frequency in the HDDs. As a result, the stroke of the micro-actuator can be reduced for the positioning control.

The authors calculated the effectiveness of the proposed controller design. In the calculation, the control system compensates for the disturbance including the internal vibration of the HDD and the external vibration caused by the data-server. The stroke of the micro-actuator was reduced by about 60% with comparison to the decouple controller design with keeping the positioning accuracy.

2. CHARACTERISTICS OF DUAL-STAGE ACTUATOR SYSTEM

The picture of the HDD is shown in Fig.1. The HDD is composed of the VCM, the micro actuator, suspension assemblies, magnetic heads, disks, and a spindle motor. The position signal on the disks is read by the magnetic head, and the position signal are input to the digital signal processor (DSP). The controller of the VCM and the micro actuator are designed based on frequency responses of the actuators. The symbol $P_{VCM}(s)$ is a frequency transfer function of the VCM. The symbol $P_{micro}(s)$ is a frequency transfer function of the micro actuator. The symbol s is the Laplace operator.

$$P_{VCM}(s) = \kappa_{vcm} \sum_{i=1}^{16} \frac{\alpha_{vcm-i}}{s^2 + 2\zeta_{vcm-i}\omega_{vcm-i}s + \omega_{vcm-i}^2} \quad (1)$$

$$P_{micro}(s) = \kappa_{micro} \sum_{i=1}^{7} \frac{\alpha_{micro-i}}{s^2 + 2\zeta_{micro-i}\omega_{micro-i}s + \omega_{micro-i}^2} \quad (2)$$

where, κ_{vcm} is 647.8, κ_{micro} is 6.83×10^9. In $P_{VCM}(s)$, the symbols ω_{vcm-i} and ζ_{vcm-i} are a natural frequency and damping ratio of the resonance, respectively, and α_{vcm-i} is an influence coefficient. In $P_{PZT}(s)$, $\omega_{micro-i}$ and $\zeta_{micro-i}$ are a natural frequency and damping ratio of the resonance, respectively, and $\alpha_{micro-i}$ is an influence coefficient. These parameters are listed in Tables 1 and 2. The frequency responses of $P_{VCM}(s)$ and $P_{micro}(s)$ are shown in Fig.2. The actuators have the mechanical resonances as shown in Fig.2. The control system has to compensate for the mechanical resonances. Furthermore, the control system is required to compensate for the forced vibration caused by the internal and external vibration. In this study, the amplitude spectrum of the vibration are defined as shown in Fig.3. The vibration includes the external vibration and the internal vibration: flow-induced vibration and repeatable runout. The external vibration is measured by using the data server as shown in Fig.4. The external vibration is caused by server fans or an adjacent HDD in the data server. Model of the flow-induced vibration is defined with reference to the previous study [Eguchi T (2017)]. Model of the repeatable runout is defined with reference to the HDD benchmark problem [Yamaguchi (2012)].

Table 1. Parameters in P_{vcm}

i	ω_{vcm-i}	α_{vcm-i}	ζ_{vcm-i}
1	0	1.00	0
2	$5300 \times 2\pi$	-1.00	0.02
3	$6100 \times 2\pi$	0.10	0.04
4	$6500 \times 2\pi$	-0.10	0.02
5	$8050 \times 2\pi$	0.04	0.01
6	$9600 \times 2\pi$	-0.70	0.03
7	$14800 \times 2\pi$	-0.20	0.01
8	$17400 \times 2\pi$	-1.00	0.02
9	$21000 \times 2\pi$	3.00	0.02
10	$26000 \times 2\pi$	-3.20	0.012
11	$26600 \times 2\pi$	2.10	0.007
12	$29000 \times 2\pi$	-1.50	0.01
13	$32200 \times 2\pi$	2.00	0.03
14	$38300 \times 2\pi$	-0.20	0.01
15	$43300 \times 2\pi$	0.30	0.01
16	$44800 \times 2\pi$	0.50	0.01

Table 2. Parameters in P_{micro}(s)

i	$\omega_{micro-i}$	$\alpha_{micro-i}$	$\zeta_{micro-i}$
1	$14800 \times 2\pi$	-0.005	0.025
2	$21500 \times 2\pi$	-0.01	0.03
3	$28000 \times 2\pi$	-0.10	0.05
4	$40200 \times 2\pi$	0.80	0.008
5	$42050 \times 2\pi$	0.30	0.008
6	$44400 \times 2\pi$	-0.25	0.01
7	$46500 \times 2\pi$	0.30	0.02

3. CONTROLLER DESIGN FOR DUAL-STAGE ACTUATOR SYSTEM

3.1 Decouple controller design for head positioning system

This section describes the conventional design method, namely the decoupling controller design. The block diagram of the decouple controller design is shown in Fig.5. The symbol $r(k)$ is reference signal, $e(k)$ is position error signal, $y_{VCM}(t)$ is displacement of the VCM, $y_{micro}(t)$ is displacement of the micro actuator, and $d(t)$ is the disturbance caused by the forced vibration. The symbol k is sample number, T_s is sampling time and t is time. The symbol $C_{VCM}(z)$ is a transfer function of feedback controller for the VCM, $C_{micro}(z)$ is a feedback controller for the micro actuator, and $D(z)$ is a decouple filter. The symbol H is a zero order hold and K is a positioning sensor. The symbol z^{-1} is the one sample delay operator.

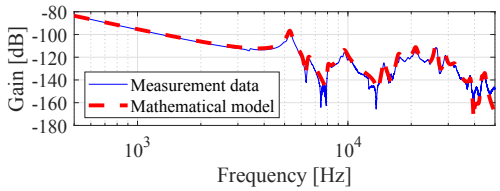

(a) $P_{VCM}(s)$

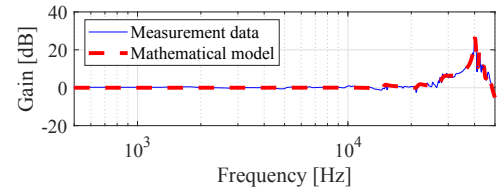

(b) $P_{micro}(s)$

Fig. 2. Frequency responses of the VCM and micro actuator

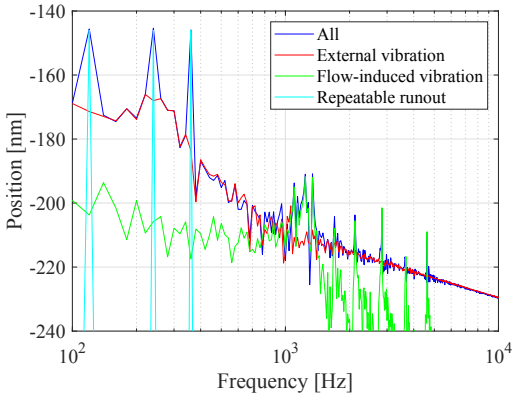

Fig. 3. Amplitude spectra of the forced vibration

When $D(z)$ is desinged as $D(z) = P_{micro}(z)$, the block diagram is re-described as Fig.6. The VCM feedback loop and the micro actuator feedback loop can be considered as connected in series. It means that $D(z)$ can decouple the interaction of the VCM and micro actuator. The sensitivity function of the decouple controller design is expressed as following equation.

$$S_{decouple}(z) = \frac{1}{1 + L_{VCM}(z)} \frac{1}{1 + L_{micro}(z)} \tag{3}$$

The symbols $P_{VCM}(z)$ and $P_{micro}(z)$ are $P_{VCM}(s)$ and $P_{micro}(s)$ discretized by the sampling time T_s for the calculation of the sensitivity function. The symbols $L_{VCM}(z) =$

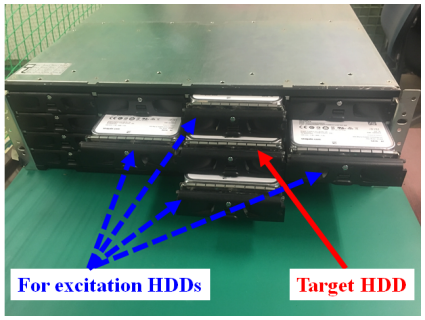

Fig. 4. Experimental system for measuring the external vibrations

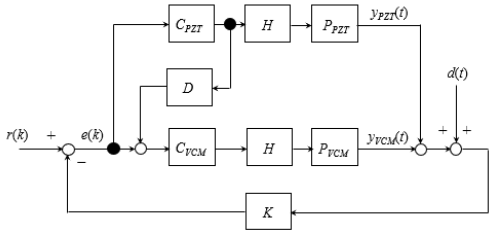

Fig. 5. Block diagram of the decouple controller design

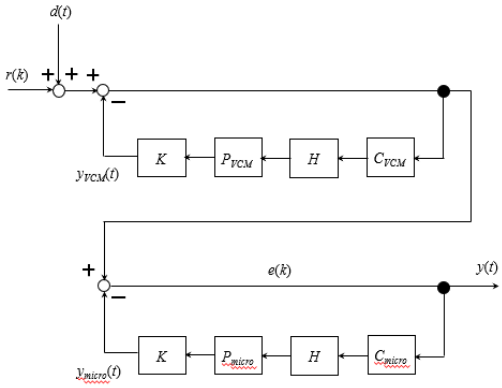

Fig. 6. Transformed block diagram of the decouple controller design

$P_{VCM}(z)C_{VCM}(z)$ and $L_{micro}(z) = P_{micro}(z)C_{micro}(z)$ are open loop of the VCM feedback loop and the micro actuator, respectively. The sensitivity function of the VCM feedback loop is $S_{VCM}(z) = \frac{1}{1+L_{VCM}(z)}$, and that of micro actuator is $S_{micro}(z) = \frac{1}{1+L_{micro}(z)}$ Therefore, eq.(3) can be rewritten as following equation.

$$S_{dual}(z) = S_{VCM}(z)S_{micro}(z) \tag{4}$$

The symbol $S_{dual}(z)$ is equivalent to the product of $S_{VCM}(z)$ and $S_{micro}(z)$. The characteristics of $S_{VCM}(z)$ and $S_{micro}(z)$ independent each other in the decoupling controller design. The design example as referred [Atsumi (2018)] are shown in Fig,7, Fig.8 and Fig.9, respectively. The designer can deal with the control system as the SISO system. It is the merit for management of the controller design; the feedback controllers can be designed independently. On the other hand, there is constraint which is each feedback loop must be stabilized in this control system.

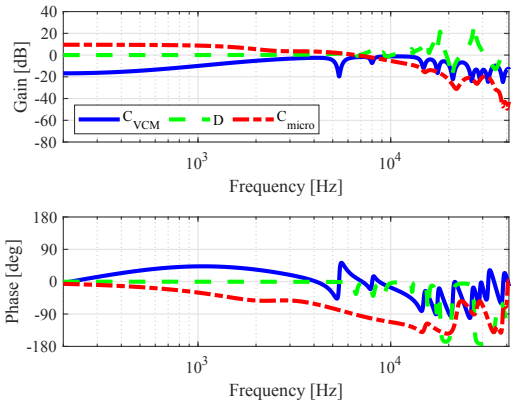

Fig. 7. Frequency responses of controller in the decouple controller design

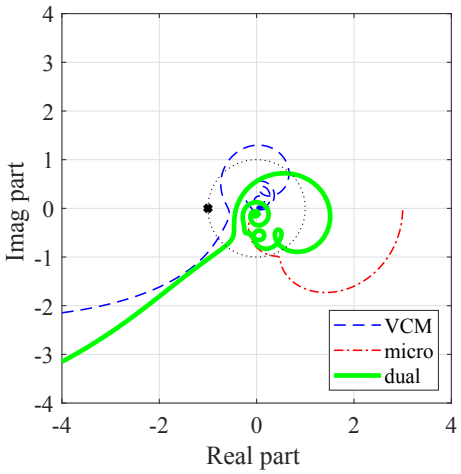

Fig. 8. Nyquist diagram of the open loop in the decouple controller design

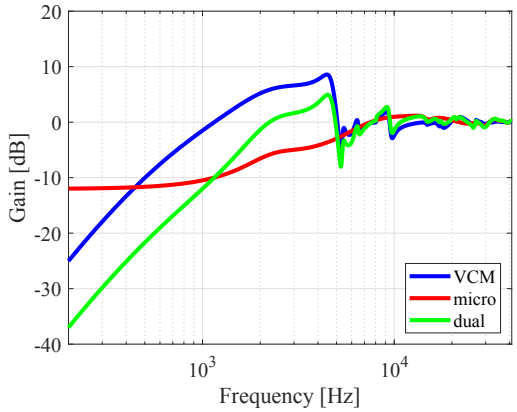

Fig. 9. Frequency responses of sensitivity function in the decouple controller design

3.2 Proposed controller design for stroke reduction of the micro actuator

The block diagram of the control system for the proposed controller design is shown in Fig.10. The decoupling filter $D(z)$ is removed in this control system, and then the sensitivity function is expressed as following equation.

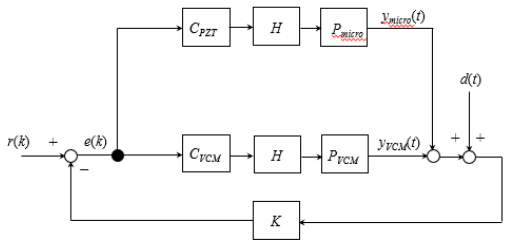

Fig. 10. Block diagram of proposed design in head positioning system of HDD

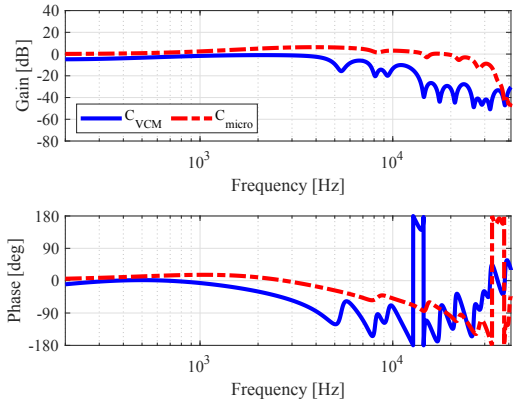

Fig. 11. Frequency responses of controller in the proposed controller design

$$S_{dual}(z) = \frac{1}{1 + L_{VCM}(z) + L_{micro}(z)} \tag{5}$$

Equation (5) indicates that the characteristics of the each feedback loop can't be separate as eq.4. The controller design can be more complicated than the decouple controller design. On the other hand, each feedback loop doesn't need to be stabilized, when the entire feedback loop is stabilized. It can expand the applicable frequency responses for $C_{VCM}(z)$ and $C_{micro}(z)$. Fig.11 indicates the frequency responses of the feedback controllers. In this design, the gain of $C_{micro}(z)$ can be decreased in the low frequency. Fig.12 indicates the vector locus of the open loop characteristics for each case. In this design, the VCM feedback loop is unstable due to the gain increasing of $C_{VCM}(z)$ as shown in Fig.7. However, the entire feedback loop is stabilized by the micro actuator feedback loop. Fig.13 indicates the frequency responses of the sensitivity functions. Although the frequency response of S_{dual} is almost same between the proposed controller design and the decouple controller design, the frequency responses of each feedback loop S_{VCM} and S_{micro} are difference in each design method. Especially, the proposed design decreases the gain of S_{micro} in below 1500Hz. Figure 3 indicates the lower the frequency, the larger the amplitude of the disturbance. The proposed design method can reduce the stroke of the micro-actuator due to the disturbance.

4. PERFORMANCE VERIFICATION OF THE PROPOSED CONTROLLER DESIGN

Firstly, the stability performance of the control system was confirmed. In the controller design of HDDs, the gain and phase margins and the maximum gain of the sensitivity function are usually evaluated [Mamun (2017)]. The major

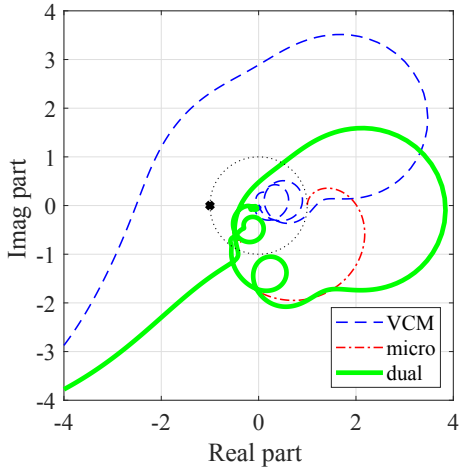

Fig. 12. Nyquist diagram of the open loop in the proposed controller design

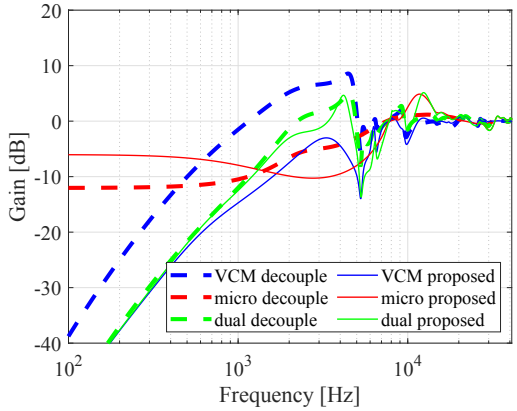

Fig. 13. Frequency responses of sensitivity function in the proposed and the decouple controller design

Table 3. Stability performance

	Gain margin	Phase margin	Max gain of $\|S\|$
VCM feedback loop			
Decouple	4.58dB	37.7 deg	8.6dB
Proposed	unstable	unstable	unstable
Micro actuator feedback loop			
Decouple	20.0dB	112.31 deg	1.1dB
Proposed	19.2dB	57.7 deg	5.1dB
entire feedback loop			
Decouple	7,54dB	50.71 deg	5.0dB
Proposed	6.93dB	56.20 deg	5.1dB

difference between the proposed method and the decouple controller design is that the VCM feedback loop must be stabilized or not. The decouple controller design, the stability criteria: the gain margin $\geq$ 4dB, the phase margin $\geq$ 30deg and the maximum sensitivity function gain $\leq$ 10dB. should be satisfied for the VCM feedback loop. On the other hand, the proposed controller design only needs to satisfy the stability criteria: gain margin $\geq$ 6dB, phase margin $\geq$40deg and the maximum sensitivity function gain $\leq$ 7dB for the entire feedback loop. The stability performance of the design result is shown in Table.3. Although the VCM feedback loop is unstable in the proposed controller design, the entire feedback loop satisfies the stability criterion.

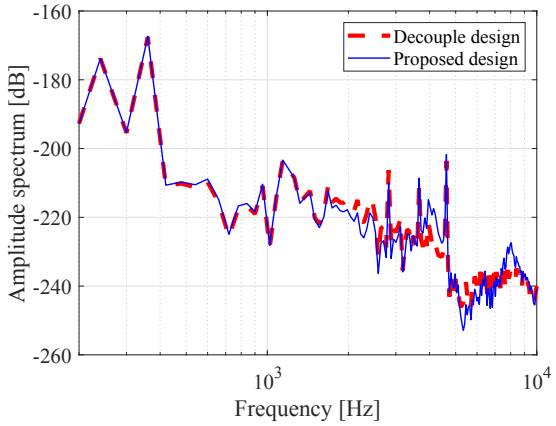

Fig. 14. Amplitude spectrum of the position error signal $e(k)$

Table 4. Sigma of the position error signal and stroke

	Decouple	Proposed
sigma of $e(k)$	3.36nm	3.38nm
sigma of $y_{vcm}(k)$	32.27nm	134.17nm
sigma of $y_{micro}(k)$	9.83nm	3.64nm

Secondary, the positioning performance of the control system was confirmed. The disturbance $d(t)$ as shown in Fig.3 was input to the control system. The amplitude spectra of the position error signal $e(k)$ were measured to evaluate the positioning accuracy, and the results are shown in Fig.14. The amplitude spectra indicate that the positioning accuracy is almost same in both design methods.

Finally, the stroke of the micro-actuator was confirmed. The amplitude spectra of the displacement $y_{VCM}(t)$ and $y_{micro}(t)$ were measured to evaluate the stroke for each actuator. The amplitude spectra for $y_{VCM}(t)$ and $y_{micro}(t)$ are shown in Fig.15. Figure 15 indicate the amplitude spectrum of $y_{VCM}(t)$ for the proposed controller design is larger than that ot the decoupling controller design in the low frequency. It comes from the increasing the gain of C_{VCM} in the proposed controller design. On the other hand, the amplitude spectrum of $y_{micro}(t)$ for the proposed controller design is smaller than that ot the decoupling controller design in the low frequency. It comes from the decreasing the gain of C_{micro} in the proposed controller design. Moreover, the step responses of $y(k)$ and $y_{micro}(t)$ are indicated in Fig.16. The position of the magnetic head is moved from 0nm to 50nm at 0.05s. The time responses of both methods are almost same, and the amplitude $y_{micro}(t)$ of the proposed method is smaller than that of the decouple controller design.

The values of sigma (standard deviation) for $e(k)$, $y_{VCM}(t)$ and $y_{micro}(t)$ are shown in Table.4. From Table.4, the sigma of $e(k)$ is almost same value, and the sigma of $y_{micro}(t)$ is decreased by about 60%. As a result, the proposed controller design can reduce the stroke of the micro actuator is about 60% with comparison to the decouple controller design.

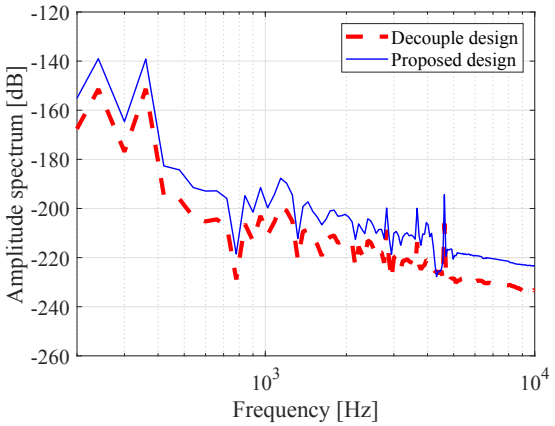

(a) for $y_{vcm}(t)$

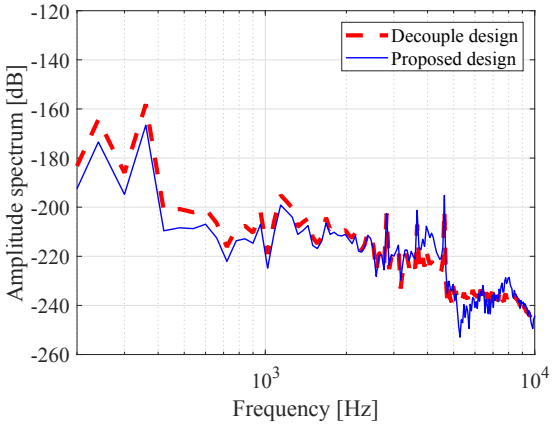

(b) for $y_{micro}(t)$

Fig. 15. Amplitude spectrum of the stroke

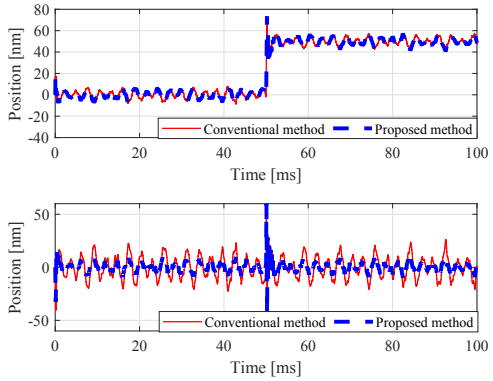

Fig. 16. Step responses of $y(k)$ (upper figure) and $y_{micro}(t)$ (low frequency)

5. CONCLUSION

In this study, we have designed the controller for stroke reduction of the micro actuator in the dual-stage actuator system of HDDs. The proposed design can expand the design possibility of the feedback controller with compensation to the conventional design, namely the decoupling controller design. The positioning accuracy and the stroke of the control system were verified during the compensation of the mixture of the internal and external disturbance in HDDs. As the results, the stroke of the micro actuator was decreased by about 60% with comparison to the decoupling controller design. The reduction can be realized by increasing the controller gain of VCM. The proposed design can balance flexibly of the stroke for each actuator by adjusting the feedback controller gains.

REFERENCES

Atusmi T. Two-degree-of-freedom control scheme for flying-height and tracking-position controls with thermal actuators in HDDs. *Journal of Advanced Mechanical Design, Systems, and Manufacturing*, Vol.12, No.1, 15pages, 2018.

Atsumi T. and Yabui S. Quadruple-Stage Actuator System for Magnetic-Head Positioning System in HDDs, *IEEE Transactions on Industrial Electronics* doi: 10.1109/TIE.2019.2955432

Bashash, S. and Shariat S. Performance enhancement of hard disk drives through data-driven control design and population clustering. *Precision Engineering*, Available online 17 December 2018

Bettiol M., Capestro M. and Di Maria (2017). Industry 4.0: the strategic role of marketin. , URL: www.economia.unipd.it/sites/economia.unipd.it/files/20170213.pdf

Bhushan, B, Springer Handbook of Nanotechnology, *Springer Hand books* ISBN 978-3-540-29838-0, 2004.

Eguchi T. Characteristics of Disk Flutter in Mixture Gas of Helium and Air. *Proceedings of conference on Information, Intelligence and Precision Equipment*, B-04, 2017.

HGST (2017). TECH BRIEF: HGST Micro Actuator. *TB02-HGST-Mico-Actuator-EN-US-0917-0*, URL: https://www.westerndigital.com/.

Ito J and Atsumi T. Controller Design Method for Dual-Stage-Actuator System of HDDs by using RBode Plot. *Proceedings of the 4th IEEJ International Workshop on Sensing, Actuation, Motion Control, and Optimization*, TT6–3, 2018.

Kobayashi M., Nakagawa S. and Numasato H. Adaptive Control of Dual-Stage Actuator for Hard Disk Drives. *Proceeding of the 2004 American Control Conference*, pp. 523-528, 2004.

Mamun A A., Guo G. and Bi C. Hard Disk Drive: Mechatronics and Control. *CRC Press*, 2017.

Mamun A A., Guo G. and Bi C. Digital Data Storage Outlook 2017. , URL: https://spectralogic.com/wp-content/uploads/white-paper-digital-data-storage-outlook-2017-v3.pdf.

Yabui S., Atsumi T. and Inoue T. Coupling controller design for MISO system of head positioning control systems in HDDs *IEEE Transactions on Magnetics* doi: 10.1109/TMAG.2020.2978156

Yamaguchi T., Hirata M. and Pang C.K. High-speed precision motion control. *CRC Press*, 2012.

Yamato Y. Cloud Storage Application Area of HDD-SSD Hybrid Storage, Distributed Storage, and HDD Storage. *IEEJ TRANSACTIONS on Electrical and Electronic Engineering*, Vol. 11, pp. 674-675, 2016.